



ISTITUTO NAZIONALE DI RICERCA METROLOGICA Repository Istituzionale

Low-temperature spectroscopy of the $12\text{C}_2\text{H}_2$ ($\nu_1+\nu_3$) band in a helium buffer gas

This is the author's submitted version of the contribution published as:

Original

Low-temperature spectroscopy of the $12\text{C}_2\text{H}_2$ ($\nu_1+\nu_3$) band in a helium buffer gas / Santamaria, L; Di Sarno, V; Ricciardi, I; De Rosa, M; Mosca, S; Santambrogio, Gabriele; Maddaloni, P; De Natale, P.. - In: THE ASTROPHYSICAL JOURNAL. - ISSN 0004-637X. - 801:(2015), p. 50.50. [10.1088/0004-637X/801/1/50]

Availability:

This version is available at: 11696/29015 since: 2021-03-02T17:27:24Z

Publisher:

The American Astronomical Society

Published

DOI:10.1088/0004-637X/801/1/50

Terms of use:

This article is made available under terms and conditions as specified in the corresponding bibliographic description in the repository

Publisher copyright

Institute of Physics Publishing Ltd (IOP)

IOP Publishing Ltd is not responsible for any errors or omissions in this version of the manuscript or any version derived from it. The Version of Record is available online at DOI indicated above

(Article begins on next page)

Low-temperature spectroscopy of the $^{12}\text{C}_2\text{H}_2$ ($\nu_1 + \nu_3$) band in a helium buffer gas

L. Santamaria¹, V. Di Sarno¹, I. Ricciardi¹, M. De Rosa¹,
S. Mosca¹, G. Santambrogio^{2,3}, P. Maddaloni^{1,4}, and
P. De Natale^{4,5}

¹ CNR-INO, Istituto Nazionale di Ottica, Via Campi Flegrei 34, 80078 Pozzuoli, Italy

² CNR-INO, Istituto Nazionale di Ottica, Via N. Carrara 1, 50019 Sesto Fiorentino, Italy

³ Fritz-Haber-Institut der Max-Planck-Gesellschaft, Faradayweg 4-6, 14195 Berlin, Germany

⁴ INFN, Istituto Nazionale di Fisica Nucleare, Sez. di Firenze, Via G. Sansone 1, 50019 Sesto Fiorentino, Italy

⁵ CNR-INO, Istituto Nazionale di Ottica, Largo E. Fermi 6, 50125 Firenze, Italy

E-mail: pasquale.maddaloni@ino.it

October 2014

Abstract. Buffer gas cooling with a ^4He gas is used to perform laser-absorption spectroscopy of the $^{12}\text{C}_2\text{H}_2$ ($\nu_1 + \nu_3$) band at cryogenic temperatures. Doppler thermometry is first carried out to extract translational temperatures from the recorded spectra. Then, rotational temperatures down to 20 K are retrieved by fitting the Boltzmann distribution to the relative intensities of several ro-vibrational lines. The underlying helium-acetylene collisional physics, relevant for modeling planetary atmospheres, is also addressed. In particular, the diffusion time of $^{12}\text{C}_2\text{H}_2$ in the buffer cell is measured against the ^4He flux at two separate translational temperatures; the observed behavior is then compared with that predicted by a Monte Carlo simulation, thus providing an estimate for the respective total elastic cross sections: $\sigma_{el}(100\text{ K}) = (4 \pm 1) \cdot 10^{-20}\text{ m}^2$ and $\sigma_{el}(25\text{ K}) = (7 \pm 2) \cdot 10^{-20}\text{ m}^2$.

Keywords: Buffer gas cooling, Cold ^4He – $^{12}\text{C}_2\text{H}_2$ collisions, Laser-absorption ro-vibrational spectroscopy.

Submitted to: *The Astrophysical Journal*

1. Introduction

By virtue of its prototypical role in different research areas, acetylene has been the subject of extensive spectroscopic studies [1, 2]. First, the paradigmatic carbon-carbon triple bond provides a fertile ground for the exploration of fundamental quantum

chemistry processes in molecular beams, including reactions and collisions as well as the formation of van der Waals complexes [3, 4, 5]. From a technological perspective, much work in the field of high-resolution spectroscopy has been motivated by the demand for improved frequency standards and metrological capabilities in the telecom spectral region [6, 7, 8, 9]. Moreover, trace-molecule spectroscopy of acetylene is of considerable interest in atmospheric chemistry and geophysical research in connection with pollution control and global climate, respectively [10]. While representing only a trace component on Earth, acetylene is formed, by photolysis of methane, in the atmospheres of jovian planets (Jupiter, Saturn, Uranus, and Neptune) and Titan, as well as in various other stellar and interstellar environments [11, 12, 13]; as such, acetylene is also a key species in astrophysics and astrobiology [14].

Potentially profitable in all the above applications, laboratory spectroscopy investigations of acetylene in the low-temperature regime are crucial to understand and model planetary atmospheres. Indeed, it was thanks to the $^{12}\text{C}_2\text{H}_2$ ro-vibrational emission spectra at $13.7\ \mu\text{m}$ (ν_5 -fundamental band) observed by the instruments on board *Voyagers 1* and *2* that the atmospheric temperature of Jupiter (about 130 K), Titan (between 120 and 130 K), Saturn (around 90 K) and Neptune (below 60 K) were retrieved [15]. More recently, infrared spectroscopic measurements performed by the Spitzer Space Telescope discovered trace amounts of acetylene in the troposphere of Uranus as well, consistent with a lowest recorded temperature of 49 K [16]. While spectral lines in planetary atmospheres are mainly influenced by collisions with molecular hydrogen, atomic helium plays an important role, too. In this regard, calculations and measurements of collisional broadening and shift coefficients were specifically carried out for the helium-acetylene system, first on the mid-infrared ($\nu_4 + \nu_5$) [17] and ν_5 [18, 15, 19, 20] bands, respectively at 7.4 and $13.7\ \mu\text{m}$, and then on the near-infrared ($\nu_1 + 3\nu_3$) [21] and ($\nu_1 + \nu_3$) [22, 23, 24] bands, at $788\ \text{nm}$ and $1.5\ \mu\text{m}$, respectively; however, most of these studies focused on room-temperature systems, except for a couple of works reporting temperatures just below 195 [24] and 150 [17] K. The general difficulty encountered in accessing the range of tens of Kelvin with laboratory spectroscopic setups lies in the fact that most of the species of interest, including acetylene, have poor vapor pressure in that temperature interval. Only in very few cases, based on a special collisional cooling methodology, was such a limitation overcome and significantly lower temperatures, down to 4 K, reached [25]. This allowed comprehensive investigations of pressure broadening in the CO-He system [25], He-induced rotational relaxation of H_2CO [26], and rotational inelastic cross sections for H_2S -He collisions [27]. Nevertheless, this approach has never been applied to acetylene.

A new impetus to this research line comes from the emerging, powerful technologies for the cooling of stable molecules [28]. Among the various schemes, at least for temperatures in the few-Kelvin range, the buffer-gas-cooling (BGC) method is perhaps the most efficient in terms of produced sample density and it is applicable to nearly all molecules [29, 30]. Here, a noble gas, typically helium, is chilled just above its boiling point and acts as a thermal bath (buffer) that cools in turn, through collisions, the

injected molecular gas under analysis.

In this work, a BGC apparatus with ^4He (boiling point of $\simeq 4.2$ K at 1 atm) is used to prepare a $^{12}\text{C}_2\text{H}_2$ (boiling point of $\simeq 190$ K at 1 atm) sample at temperatures which are characteristic of planetary atmospheres and the interstellar medium. In this regime, laser absorption spectroscopy is performed, primarily aimed at determining, in conjunction with the outcomes of a Monte Carlo simulation, the total (as opposed to differential) elastic cross sections for the ^4He – $^{12}\text{C}_2\text{H}_2$ system. For this purpose, a thorough characterization of the BGC process is first accomplished, comprising measurements of translational temperatures by means of Doppler thermometry, as well as of internal (rotational) temperatures through the analysis of the relative intensities of several rotational lines.

2. Experimental setup

Described in detail in a previous work [31], the heart of the experimental apparatus is represented by a two-stage pulse tube (PT) cryocooler (Cryomech, PT415) housed in a stainless-steel vacuum chamber and fed with liquid helium by a compressor. The first (second) PT stage yields a temperature of 45 K (4.2 K) provided that its heat load is kept below 40 W (1.5 W); to guarantee this, each plate is enclosed in a round gold-plated copper shield, which suppresses black-body radiation effects. Capillary filling, regulated upstream by two flow controllers with an accuracy of 0.05 Standard Cubic Centimeters per Minute (SCCM), is used to inject both acetylene and helium, contained in room-temperature bottles, into the buffer cell. This latter consists of a gold-plated copper cube of side length $L_c = 54$ mm; it is in thermal contact with the 4.2-K plate and its exit hole has a radius of $r_h = 1$ mm. The acetylene pipe is made of stainless-steel and thermally insulated from both the PT stages; in addition, to avoid condensation, its temperature is maintained above 190 K by means of a proportional-integral-derivative (PID) feedback loop equipped with a silicon-diode thermometer as input sensor and an electric heater as output transducer. The buffer gas line comprises four connected segments: the first one is made of stainless-steel and consists of several windings in order to keep the heat conductance as low as possible; then, a bobbin-shaped copper tube is secured to the 45-K plate; the third segment, identical to the first duct, minimizes thermal exchanges between the two PT stages; finally, a second spool-shaped copper pipe is fixed to the 4.2-K plate, intended to cool the helium gas down to a few K before entering the buffer cell. A second PID controller is also implemented for fine tuning of the buffer cell temperature. To keep the pressure within the radiation shields below 10^{-7} mbar, the internal surface of the inner shield is covered with a layer of activated charcoal that, at cryogenic temperatures, acts as a pump (with a speed of a few thousands dm^3/s) for helium and non-guided molecules; the gas adsorbed by the charcoal is released during warm up of the cryogenic system and then pumped out of the vessel by a turbomolecular pump. As shown in Fig. 1, both the vacuum chamber, the shields and the buffer cell have optical accesses for spectroscopic interrogation. The probe radiation source is an

external-cavity (Littman-Metcalf configuration) diode laser emitting several milliwatts of power between 1520 and 1570 nm with a linewidth below 1 MHz (New Focus, TLB-6300 Velocity). The laser output beam is split into four parts: one portion is sent to a room-temperature cell containing acetylene in order to identify the various transitions; a second beam is coupled to a confocal, Fabry-Perot (FP) interferometer for frequency calibration purposes; a third fraction is delivered to a wavelength meter with an accuracy of 0.2 ppm (Burleigh WA-1500); the last part passes through the buffer gas cell and is eventually collected by an InGaAs photo-detector (PD). The molecular absorption profile, $\delta(\nu) \equiv [I_0 - I(\nu)]/I_0$, is recovered by scanning the laser frequency ν through the application of a linear-ramp voltage to the piezoelectric transducer attached to the external-cavity tuning element.

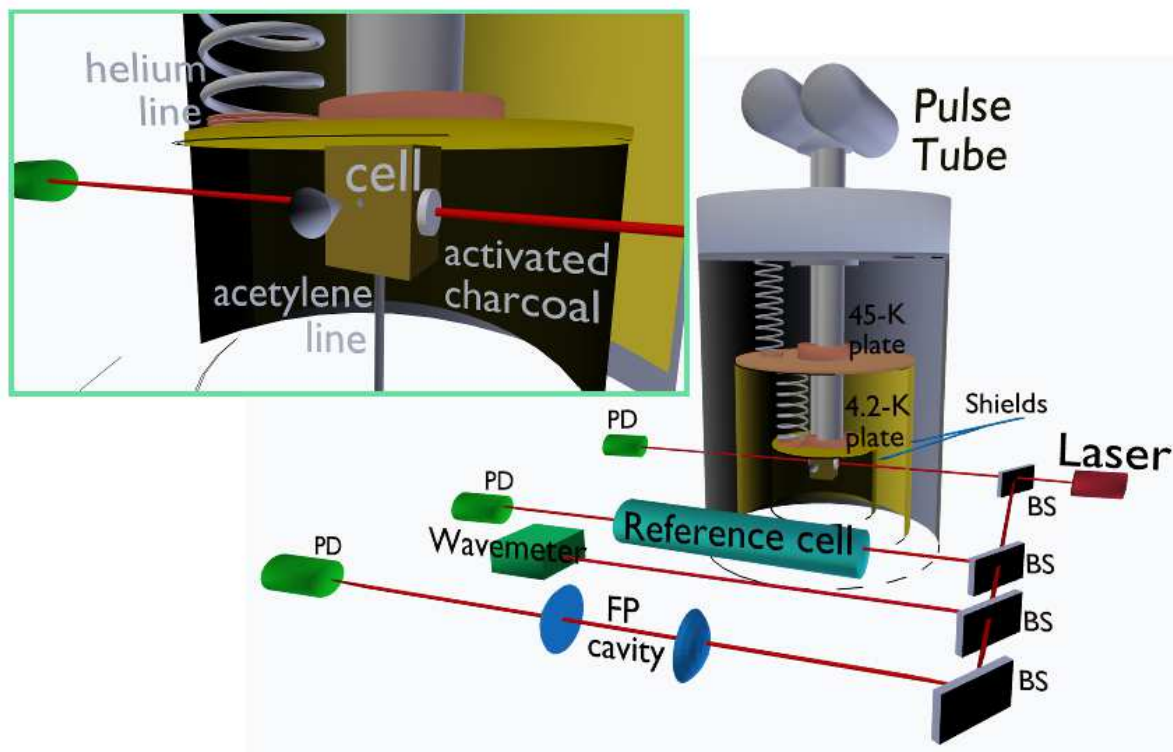


Figure 1. Layout of the experimental setup including a zoom on the buffer-gas cell. Laser absorption spectroscopy is used to characterize collisional cooling of $^{12}\text{C}_2\text{H}_2$ in a ^4He thermal bath down to a temperature of few Kelvin.

3. Measurements and analysis

3.1. Translational temperatures

In order to monitor the collisional cooling process, the absorption spectrum of the R(5) ro-vibrational transition in the ($\nu_1 + \nu_3$) band (henceforth referred to as transition *a*) was acquired under different experimental conditions, by varying the buffer-cell temperature, T_{cell} , and the two gas flows, f_{He} and $f_{\text{C}_2\text{H}_2}$. Since the translational temperature, T_{trans} ,

in a gas is related to the mean square velocity of its molecules, each observed absorption profile was fitted by a Gaussian distribution

$$G(\nu) = G_0 \exp \left[-\frac{4 \ln 2 (\nu - \nu_0)^2}{\sigma_D^2} \right] \quad (1)$$

where the amplitude G_0 , the transition center frequency ν_0 , and the Doppler width $\sigma_D = (\nu_0/c)\sqrt{8 \ln 2 m^{-1} k_B T_{trans}}$ represent the fitting parameters (here, m is the molecular mass, c the light speed, and k_B the Boltzmann constant). Thus, the translational temperature of the acetylene sample was retrieved by the extracted σ_D value. As an example, three absorption spectra are shown in Fig. 2, corresponding to the following T_{cell} values: 294, 115 and 10 K; for $T_{cell} = 294$ K, only 1 SCCM of acetylene was let into the cell and no helium; for $T_{cell} = 115$ K, $f_{\text{He}} = 20$ SCCM and $f_{\text{C}_2\text{H}_2} = 5$ SCCM were used; for $T_{cell} = 10$ K, $f_{\text{He}} = f_{\text{C}_2\text{H}_2} = 2$ SCCM was found to be the optimal choice to reach the translationally coldest sample with our setup: $T_{trans} = 15 \pm 3$ K. Supported by a temperature reading of 15 K recorded on the He pipe just before the entrance into the buffer cell, the discrepancy at the lowest temperature was attributed to a non-perfect thermal exchange between the copper pipe and the two PT plates; to bridge this gap, an improved setup for better cooling of the He line is already under construction. It should be noted that equal flows of the two gases do not correspond to equal densities in the buffer cell. In fact, many of the acetylene molecules freeze upon impact on the walls (as well as on the optical windows), hence generating a layer of solid acetylene whose thickness increases with time. This is not the case for the helium. Nonetheless, after a short transient (less than 10 ms in the worst case), stationary gas densities, n_{He} and $n_{\text{C}_2\text{H}_2}$, namely gas pressures, will be established inside the buffer cell, leading to steady-state spectroscopic absorption profiles; these will eventually disappear as soon as the optical windows fog up. It is also worth remarking here that, in the work presented here, the stationary cell gas pressures were always lower than 0.2 mbar, giving rise to negligible pressure broadening and shift effects [24].

3.2. Rotational temperatures

The linestrength of a given ro-vibrational transition depends on the rotational temperature, T_{rot} , hereafter simply called T to simplify the notation, through the relationship [32]

$$S(T) = S(T_{ref}) \frac{Q(T_{ref})}{Q(T)} \frac{\exp\left(\frac{-c_2 E_f}{T}\right) \left[1 - \exp\left(\frac{-c_2 \nu_0}{T}\right)\right]}{\exp\left(\frac{-c_2 E_f}{T_{ref}}\right) \left[1 - \exp\left(\frac{-c_2 \nu_0}{T_{ref}}\right)\right]}, \quad (2)$$

where T_{ref} is a reference rotational temperature at which the linestrength is known, $Q(T)$ the rotational partition function (varying between 3 at 10 K and 100 at 294 K in the case of acetylene [33]), E_f the transition's lower-level energy (expressed in wavenumbers), and $c_2 = hc/k_B$ (h is the Plank constant). Eq. 2 was exploited to perform accurate measurements of rotational temperatures according to the following procedure. First, besides transition a (at $\nu_{0a} = 6570.042687 \text{ cm}^{-1}$), the ($\nu_1 + \nu_3$) R(1)

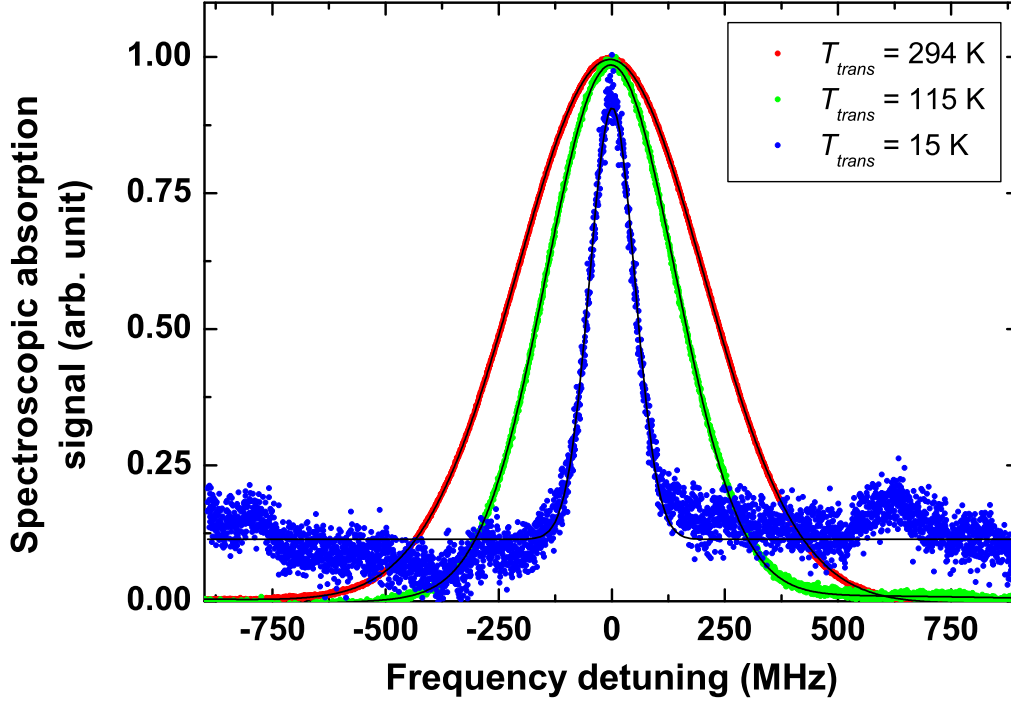


Figure 2. Spectroscopic absorption signals (normalized to unit) obtained for transition a in correspondence with the following triplets: $T_{cell} = 294$, $f_{\text{He}} = 0$ SCCM, $f_{\text{C}_2\text{H}_2} = 1$ SCCM; $T_{cell} = 115$, $f_{\text{He}} = 20$ SCCM, $f_{\text{C}_2\text{H}_2} = 5$ SCCM; $T_{cell} = 10$, $f_{\text{He}} = 2$ SCCM, $f_{\text{C}_2\text{H}_2} = 2$ SCCM. The extracted translational temperatures are: 294 ± 2 , 115 ± 5 , 15 ± 3 K, respectively.

component, called transition b (at $\nu_{0b} = 6561.094106 \text{ cm}^{-1}$), was also selected so that the ratio between the two respective linestrengths,

$$R_{ba}(T) \equiv \frac{S_b(T)}{S_a(T)} = \frac{\frac{\exp\left(\frac{-c_2 E_{fb}}{T}\right)}{\exp\left(\frac{-c_2 E_{fb}}{T_{ref}}\right)} \frac{1 - \exp\left(\frac{-c_2 \nu_{0b}}{T}\right)}{1 - \exp\left(\frac{-c_2 \nu_{0b}}{T_{ref}}\right)}}{\frac{\exp\left(\frac{-c_2 E_{fa}}{T}\right)}{\exp\left(\frac{-c_2 E_{fa}}{T_{ref}}\right)} \frac{1 - \exp\left(\frac{-c_2 \nu_{0a}}{T}\right)}{1 - \exp\left(\frac{-c_2 \nu_{0a}}{T_{ref}}\right)}}, \quad (3)$$

exhibits a steep slope below a few tens of Kelvin (see Fig. 3), thus reducing errors in the determination of low rotational temperatures. Second, for different T_{trans} values, the experimental value of $R_{ba}(T) \equiv S_b(T)/S_a(T) = \int \delta_b(\nu) d\nu / \int \delta_a(\nu) d\nu$ was determined. This value, along with the E_f 's and ν_0 's parameters provided by the Hitran database [34], was replaced in Eq. 3 which was finally solved for T (see Fig. 4). In conclusion, the minimum observed rotational temperature was $T = (20 \pm 1)$ K for a measured translational temperature of $T_{trans} = (15 \pm 3)$ K; such a difference is compatible with the fact that cooling is more efficient for the translational degrees of freedom than for

rotational ones [35], albeit the two measured temperature values are consistent within 2 standard deviations.

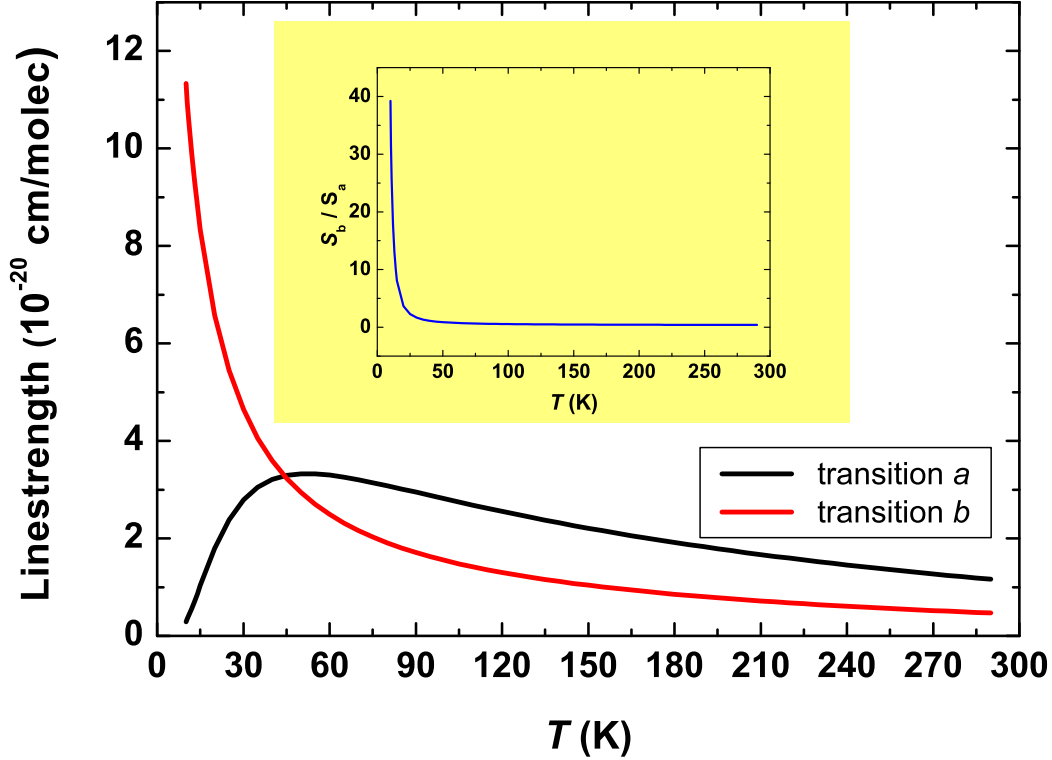


Figure 3. Linestrengths of a and b transitions, calculated using Eq. 2, are plotted as functions of rotational temperature. The ratio between the two curves is plotted in the inset.

In general, unlike what happens to translational states, even if the initial distribution over the rotational states is Boltzmannian, it will relax without preserving the canonical invariance, and it will not be possible to define a rotational temperature [36]. The necessary conditions so that the canonical invariance is maintained in a subsystem-reservoir relaxation process have been both mathematically and physically established [37]. To address this issue in our case, a normalized linestrength was measured for several ro-vibrational lines at a given translational temperature. The acquired behavior was then compared with the theoretical line dictated by the Boltzmann law. In practice, as shown in Fig. 5, the ratio $R(E_f, T) \equiv S(E_f, T)/S(E_f, T_{ref}) = \int \delta(E_f, T, \nu) d\nu / \int \delta(E_f, T_{ref}, \nu) d\nu$ was determined against E_f (i.e., for each of the transitions listed in Table 1) in correspondence with two different T_{trans} values, 19 and 28 K. It is worth pointing out that the normalization of $S(E_f, T)$ to $S(E_f, T_{ref})$ was necessary in order to get rid of the unknown dependence of $S(T_{ref})$

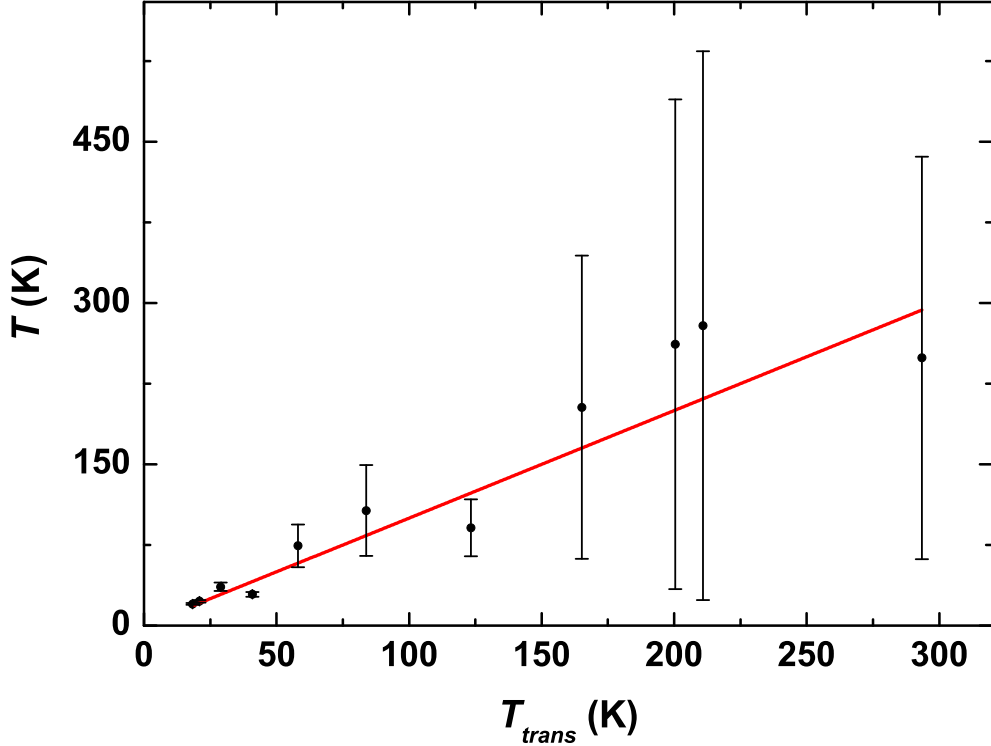


Figure 4. Experimental rotational temperatures measured at different T_{trans} values according to the procedure described in the text. The line $T = T_{trans}$ is also plotted for reference. It should be noted that each data point corresponds to a different choice of the two gas flows, essentially intended to maximize the signal-to-noise ratio of every absorption spectrum while reaching the lowest possible rotational temperature.

on E_f . The obtained data points were then fitted with the function

$$R(E_f, T) = H \exp \left[c_2 E_f \left(-\frac{1}{T} + \frac{1}{T_{ref}} \right) \right], \quad (4)$$

with H a proportionality constant, T being the fitting parameter. The above equation is nothing but Eq. 2 with $\left[1 - \exp \left(\frac{-c_2 \nu_0}{T} \right) \right] \left[1 - \exp \left(\frac{-c_2 \nu_0}{T_{ref}} \right) \right]^{-1} \simeq 1$. The extracted rotational temperatures were $T = (27 \pm 2)$ K and $T = (42 \pm 3)$ K for measured translational temperatures $T_{trans} = (19 \pm 2)$ K and $T_{trans} = (28 \pm 2)$ K, respectively. In both cases, the fit correlation coefficient was $\chi = 0.98$, consistent with the hypothesis of canonical invariance.

3.3. Elastic cross section

Finally, by comparing the measured diffusion time of $^{12}\text{C}_2\text{H}_2$ in the BGC cell (vs the ^4He flux) with that predicted by a Monte Carlo simulation, we provided an estimate for the

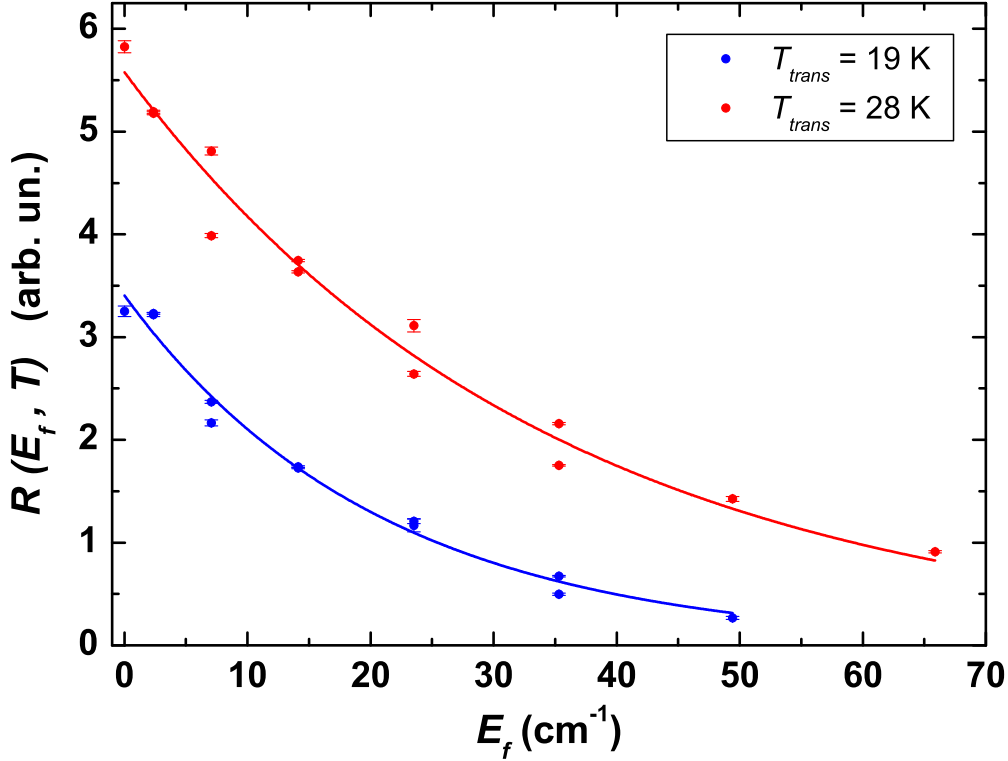


Figure 5. Ascertainment of the canonical-invariance hypothesis. Eq. 4 is fitted to the $R(E_f, T)$ data points measured as a function of the transition’s lower-level energy for two different translational temperatures (19 ± 2 and 28 ± 2 K). The extracted rotational temperatures are 27 ± 2 and 42 ± 3 K, respectively, with a fit correlation coefficient of $\chi = 0.98$. Again, as in Fig. 4, each data point is associated with a different pair of gas flows.

elastic cross section relevant to the translational cooling mechanism [39, 40]. Let us start by looking a little more closely at the physics of the problem. After reaching thermal equilibrium with the He bath (under our typical experimental conditions, this happens on a path shorter than $100 \mu\text{m}$, corresponding to about 50 collisions), a generic acetylene molecule experiences a random walk, scattered by helium atoms, until it freezes on the cell’s walls or escapes through the exit hole (to form the molecular beam); in both cases, it stops contributing to the laser absorption. The larger the helium density, the higher the number of scattering events and the longer the acetylene average diffusion time, τ_{diff} .

This latter quantity was experimentally determined for transition *a* via the

Table 1. Frequencies and lower-level energies of the ro-vibrational lines used throughout this work, as provided by the Hitran Database [34].

| E_f (cm $^{-1}$) | ν_0 (cm $^{-1}$) | J and branch |
|---------------------|-----------------------|-----------------|
| 35.2979 | 6570.042687 | R(5) $\equiv a$ |
| 23.5323 | 6567.844393 | R(4) |
| 14.1195 | 6565.620174 | R(3) |
| 7.0598 | 6563.370066 | R(2) |
| 2.3533 | 6561.094106 | R(1) $\equiv b$ |
| 0 | 6558.792333 | R(0) |
| 2.3533 | 6554.111497 | P(1) |
| 7.0598 | 6551.732512 | P(2) |
| 14.1195 | 6549.327869 | P(3) |
| 23.5323 | 6546.897607 | P(4) |
| 35.2979 | 6544.441767 | P(5) |
| 49.4163 | 6541.960389 | P(6) |
| 65.8871 | 6539.453516 | P(7) |

relationship

$$\tau_{diff}(T_{trans}) = \frac{L_c^3 n_{\text{C}_2\text{H}_2}(T_{trans})}{f_{\text{C}_2\text{H}_2}} = \frac{L_c^3}{f_{\text{C}_2\text{H}_2}} \frac{\sigma_D(T_{trans}) \int \delta_a(\nu, T_{trans}) d\nu}{S_a(T) L_c}, \quad (5)$$

where the spectroscopic derivation of the acetylene density (based on the Lambert-Beer law) was also used [35]. Then, the $S_a(T)$ value corresponding to the measured $\sigma_D(T_{trans})$ was calculated by means of Eq. 2, with E_f , ν_0 , and $S_a(T_{ref} = 294 \text{ K}) = 1.13 \cdot 10^{-20} \text{ cm/molec}$ taken from the Hitran Database, and $Q(T)$ provided by Amyay and coworkers [33]. It should be noted that, in the above procedure, $T = T_{trans}$ was inevitably assumed. To fix that, curve *a* in Fig. 3 was used to estimate the extent to which the discrepancy between T and T_{trans} (as measured in Fig. 4) affects the determination of $S_a(T)$; this is reflected in conservatively augmented error bars on the τ_{diff} data points.

The helium density was derived through the formula [38]

$$n_{\text{He}} = \frac{4f_{\text{He}}}{\pi r_h^2 \langle v_{\text{He}} \rangle}, \quad (6)$$

with $\langle v_{\text{He}} \rangle = \sqrt{8k_B T_{trans} \pi^{-1} m_{\text{He}}^{-1}}$ being the mean thermal velocity of helium particles (m_{He} is the helium atom mass). According to the above procedure, two sets of τ_{diff} vs n_{He} were recorded, corresponding to translational temperatures of 100 and 25 K, respectively.

In a second stage, a theoretical simulation was carried out to reproduce the measured acetylene diffusion times. In particular, the $^4\text{He}-^{12}\text{C}_2\text{H}_2$ interaction was processed by a conventional Monte Carlo method, whereas the molecule free evolution was made to follow Newton's law. Firstly, for a given translational temperature, an acetylene molecule was injected into the buffer cell at time $t = 0$ with its three velocity components extracted randomly according to the corresponding Maxwell-Boltzmann distribution. Then, the probability \mathcal{P} that an interaction occurs in the elementary

interval time δt was calculated considering the $^4\text{He}-^{12}\text{C}_2\text{H}_2$ relative velocity (v_{rel}), n_{He} , and a trial cross section (σ_{tr}): $\mathcal{P} = n_{\text{He}} \sigma_{tr} v_{rel} \delta t$. After that, a random number \mathcal{N} (between 0 and 1) was generated: if $\mathcal{N} < \mathcal{P}$, then the atom-molecule impact was allowed to take place and new random velocity components were consequently extracted; otherwise, the molecule evolved freely for a successive time interval δt . These steps were iterated for successive δt intervals until the molecule reached one of the walls: the time τ spent in the cell before freezing was accordingly calculated. The whole procedure was then repeated for a thousand injected molecules, namely the minimum allowed number which doesn't affect the simulation result; averaging over all the computed τ values eventually yielded τ_{diff} . Depending on the values of f_{He} , T_{trans} and σ_{tr} , a different time interval δt was used in the simulation. Its value was kept between 1 and 10 ns, i.e. always small enough not to alter the simulation outcome. For each of the two translational temperatures, the above simulation was carried out as a function of n_{He} , searching for the optimal pair of σ_{tr} values which strictly delimits the experimental points from above and from below. The results are shown in Fig. 6. The elastic cross sections were estimated to be $\sigma_{el}(T_{trans} = 100 \text{ K}) = (4 \pm 1) \cdot 10^{-20} \text{ m}^2$ and $\sigma_{el}(T_{trans} = 25 \text{ K}) = (7 \pm 2) \cdot 10^{-20} \text{ m}^2$.

4. Conclusion

Thanks to the implementation of a modern buffer-gas-cooling technique, the range of cryogenic temperatures for the spectroscopic study of acetylene in a helium environment was extended, with respect to previous literature, down to a few Kelvin. In order to accurately determine the achieved translational and rotational temperatures, several ro-vibrational transitions belonging to the ($\nu_1 + \nu_3$) band were used for Doppler thermometry and measurements of relative intensities. The attainment of a well-defined rotational temperature for the considered $^4\text{He}-^{12}\text{C}_2\text{H}_2$ system was also demonstrated. Finally, a deeper insight into the collisional cooling process was gained by measuring the acetylene diffusion time in the buffer cell against the helium density at two temperatures that spanned a large range (100 and 25 K); in this respect, an appropriate theoretical model was also developed, which allowed us to obtain an estimate for the respective elastic cross sections. These figures may be particularly useful in planetary science when modeling the process of translational energy relaxation of molecules in bath gases, which is crucial for understanding the energy balance of the upper atmosphere and its evolution [43, 44].

While insignificant in the range of pressures explored in this work, pressure broadening and shifts are also of foremost importance at temperatures of astrophysical relevance and, as such, will be the subject of future investigations. Moreover, accurate analysis/modeling of spectral lineshapes represents a powerful tool for probing fundamental atom-molecule low-temperature interaction processes; obtaining molecular spectra with enhanced signal-to-noise ratios is vital for addressing this issue and, indeed, work is in progress for the implementation of a cavity ring-down spectroscopy

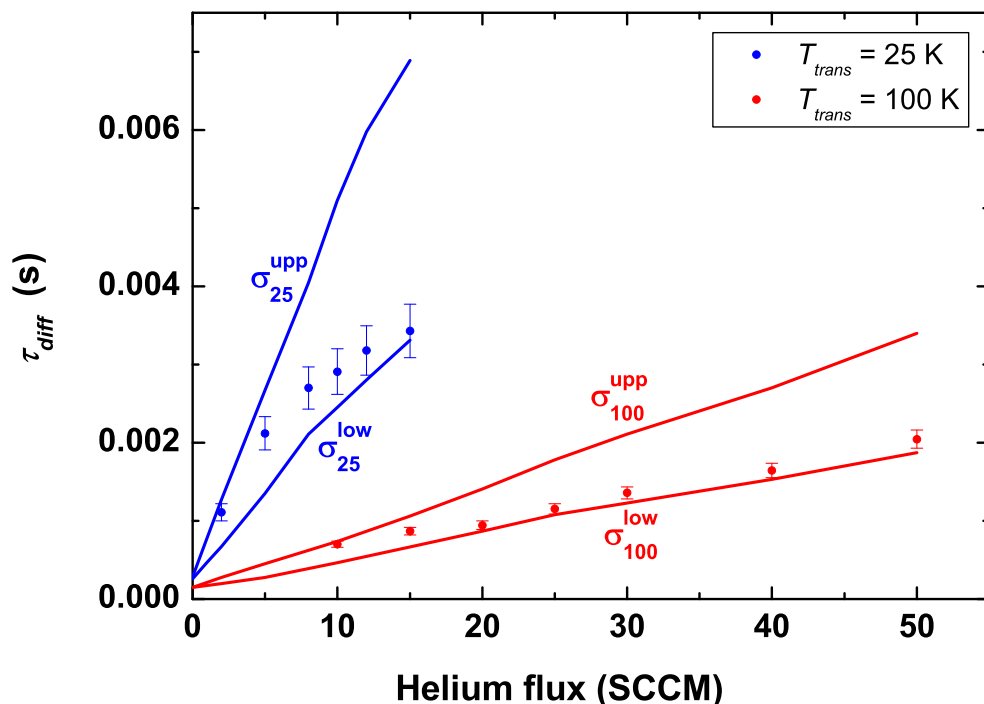


Figure 6. Experimental acetylene diffusion time plotted against f_{He} at a constant acetylene flux: $f_{\text{C}_2\text{H}_2} = 5$ SCCM for $T_{\text{trans}} = 25$ K and $f_{\text{C}_2\text{H}_2} = 50$ SCCM for $T_{\text{trans}} = 100$ K. Theoretical simulations (continuous lines) are also shown which delimit the measured data from above and from below ($\sigma_{100}^{\text{upp}} = 9.0 \cdot 10^{-20}$ m², $\sigma_{100}^{\text{low}} = 4.6 \cdot 10^{-20}$ m²; $\sigma_{25}^{\text{upp}} = 4.9 \cdot 10^{-20}$ m², $\sigma_{25}^{\text{low}} = 3.1 \cdot 10^{-20}$ m²), thus enabling the estimate of the total elastic cross sections.

technique. Finally, by virtue of the enormous versatility of our buffer-gas-cooling apparatus, the spectroscopic study reported here may be readily extended to other fundamental atmospheric and astrophysical molecular species such as, for instance, methane [45, 46], nitrous oxide [47], and carbon dioxide [42].

The authors acknowledge technical support by G. Notariale. This work was funded by MIUR-FIRB project RBFR1006TZ and by INFN project SUPREMO.

- [1] M. Herman, A. Campargue, M.I. El Idrissi, J. Vander Auwera, “Vibrational Spectroscopic Database on Acetylene, $\tilde{X}^1\Sigma_g^+$ ($^{12}\text{C}_2\text{H}_2$, $^{12}\text{C}_2\text{D}_2$, and $^{13}\text{C}_2\text{H}_2$)”, *J. Phys. Chem. Ref. Data* **32**, 921 (2003)
- [2] M. Herman, “The acetylene ground state saga”, *Molecular Physics* **105**, 2217 (2007)
- [3] F. Thibault, D. Cappelletti, F. Pirani, G. Blanquet, M. Bartolomei, “Molecular-beam scattering and pressure broadening cross sections for the acetylene-neon system” *Eur. Phys. J. D* **44**, 337

(2007)

- [4] M.J. Thorpe, F. Adler, K.C. Cossel, M.H.G. de Miranda, J. Ye, “Tomography of a supersonically cooled molecular jet using cavity-enhanced direct frequency comb spectroscopy”, *Chemical Physics Letters* **468**, 1 (2009)
- [5] K. Didriche, T. Földes, C. Lauzin, D. Golebiowski, J. Liévin, M. Herman, “Experimental 2CH excitation in acetylene-containing van der Waals”, *Molecular Physics* **110**, 2781 (2012)
- [6] C.S. Edwards, G.P. Barwood, H.S. Margolis, P. Gill, W.R.C. Rowley, “High-precision frequency measurements of the $\nu_1 + \nu_3$ combination band of $^{12}\text{C}_2\text{H}_2$ in the 1.5 μm region”, *Journal of Molecular Spectroscopy* **234**, 143 (2005)
- [7] J.L. Hardwick, Z.T. Martin, E.A. Schoene, V. Tyng, E.N. Wolf, “Diode laser absorption spectrum of cold bands of C_2HD at 6500 cm^{-1} ”, *Journal of Molecular Spectroscopy* **239**, 208 (2006)
- [8] H.Y. Ryu, S.H. Lee, W.K. Lee, H.S. Moon, H.S. Suh, “Absolute frequency measurement of an acetylene stabilized laser using a selected single mode from a femtosecond fiber laser comb”, *Optics Express* **16**, 2867 (2008)
- [9] V. Ahtee, M. Merimaa, K. Nyholm, “Precision spectroscopy of acetylene transitions using an optical frequency synthesizer”, *Optics Letters* **34**, 2619 (2009)
- [10] C.P. Rinsland, R. Zander, C.B. Farmer, R.H. Norton, J.M. Russell, “Concentrations of Ethane (C_2H_6) in the Lower Stratosphere and Upper Troposphere and Acetylene (C_2H_2) in the Upper Troposphere Deduced From Atmospheric Trace Molecule Spectroscopy/Spacelab 3 Spectra”, *Journal of Geophysical Research* **92**, 11951 (1987)
- [11] P. Varanasi, L.P. Giver, F.P.J. Valero, “Infrared absorption by acetylene in the 1214 μm region at low temperatures”, *J. Quant. Spec. Radiat Transf.* **30**, 497 (1983)
- [12] K.S. Noll, R.F. Knacke, A.T. Tokunaga, J.H. Lacy, S. Beck, E. Serabyn, “The Abundances of Ethane and Acetylene in the Atmospheres of Jupiter and Saturn”, *Icarus* **65**, 257 (1986)
- [13] B. Conrath, F.M. Flasar, R. Hanel, V. Kunde, W. Maguire, J. Pearl, J. Pirraglia, R. Samuelson, P. Gierasch, A. Weir, B. Bezaud, D. Gautier, D. Cruikshank, L. Horn, R. Springer, W. Shaffer, “Infrared Observations of the Neptunian System” *Science*, **246**, 1454 (1989)
- [14] R.S. Oremland, M.A. Voytek, “Acetylene as fast food: implications for development of life on anoxic primordial Earth and in the outer solar system”, *Astrobiology* **8**, 45 (2008)
- [15] P. Varanasi, “Intensity and lineshape measurements in the 13.7 μm fundamental bands of $^{12}\text{C}_2\text{H}_2$ and $^{12}\text{C}^{13}\text{CH}_2$ at planetary atmospheric temperatures”, *J. Quant. Spectrosc. Radiat. Transfer* **47**, 263 (1992)
- [16] M. Burgdorf, G. Orton, J. van Cleve, V. Meadows, J. Houck, “Detection of new hydrocarbons in Uranus’ atmosphere by infrared spectroscopy”, *Icarus* **184**, 634 (2006)
- [17] J.R. Podolske, M. Loewenstein, “Diode laser line strength measurements of the $(\nu_4 + \nu_5)^0$ band of $^{12}\text{C}_2\text{H}_2$ ”, *Journal of Molecular Spectroscopy* **107**, 241 (1984)
- [18] J.P. Bouanich, C. Boulet, G. Blanquet, J. Walrand, D. Lambot, “Lineshape and broadening coefficients in the ν_5 band of C_2H_2 in collision with Kr and He”, *J. Quant. Spectrosc. Radiat. Transfer* **46**, 317 (1991)
- [19] A. Babay, M. Ibrahimi, V. Lemaire, B. Lemoine, F. Rohart, J.P. Bouanich, “Line frequency shifting in the ν_5 band of C_2H_2 ”, *J. Quant. Spectrosc. Radiat. Transfer* **59**, 195 (1998)
- [20] T.G.A. Heijmen, R. Moszynski, P.E.S. Wormer, A. van der Avoird, A.D. Rudert, J.B. Halpern, J. Martin, W.B. Gao, H. Zacharias, “Rotational state-to-state rate constants and pressure broadening coefficients for HeC_2H_2 collisions: Theory and experiment”, *J. Chem. Phys.* **111**, 2519 (1999)
- [21] H. Valipour, D. Zimmermann, “Investigation of J dependence of line shift, line broadening, and line narrowing coefficients in the $\nu_1 + 3\nu_3$ absorption band of acetylene”, *Journal of Chemical Physics* **114**, 3535 (2001)
- [22] F. Thibault, “Theoretical He-broadening coefficients of infrared and Raman C_2H_2 lines and their temperature dependence”, *Journal of Molecular Spectroscopy* **234**, 286 (2005)
- [23] S.W. Arteaga, C.M. Bejger, J.L. Gerecke, J.L. Hardwick, Z.T. Martin, J. Mayo, E.A. McIlhattan,

- J.-M.F. Moreau, M.J. Pilkenton, M.J. Polston, B.T. Robertson, Wolf, “Line broadening and shift coefficients of acetylene at 1550 nm”, *Journal of Molecular Spectroscopy* **243**, 253 (2007)
- [24] K.S. Bond, N.D. Collett, E.P. Fuller, J.L. Hardwick, E.E. Hinds, T.W. Keiber, I.S.G. Kelly-Morgan, C.M. Matthys, M.J. Pilkenton, K.W. Sinclair, A.A Taylor, “Temperature dependence of pressure broadening and shifts of acetylene at 1550 nm by He, Ne, and Ar”, *Appl. Phys. B* **90**, 255 (2008)
- [25] J.K. Messer, F.C. De Lucia, “Measurement of Pressure-Broadening Parameters for the CO-He System at 4 K”, *Phys. Rev. Lett.* **53**, 2555 (1984)
- [26] C.D. Ball, F.C. De Lucia, “Direct Measurement of Rotationally Inelastic Cross Sections at Astrophysical and Quantum Collisional Temperatures”, *Phys. Rev. Lett.* **81**, 305 (1998)
- [27] M. Mengel, F.C. De Lucia, “Helium and hydrogen induced rotational relaxation of H_2CO observed at temperatures of the interstellar medium”, *The Astrophysical Journal* **543**, 271 (2000)
- [28] L.D. Carr, D. DeMille, R.V. Krems, J. Ye, “Cold and ultracold molecules: science, technology and applications”, *New Journal of Physics* **11**, 055049 (2009)
- [29] S.E. Maxwell, N. Brahm, R. deCarvalho, D.R. Glenn, J.S. Helton, S.V. Nguyen, D. Patterson, J. Petricka, D. DeMille, J.M. Doyle, “High-Flux Beam Source for Cold, Slow Atoms or Molecules”, *Phys. Rev. Lett.* **95**, 173201 (2005)
- [30] N.E. Bulleid, S.M. Skoff, R.J. Hendricks, B.E. Sauer, E.A. Hinds, M.R. Tarbutt, “Characterization of a cryogenic beam source for atoms and molecules”, *Phys. Chem. Chem. Phys.* **15**, 12299 (2013)
- [31] L. Santamaria, V. Di Sarno, I. Ricciardi, S. Mosca, M. De Rosa, G. Santambrogio, P. Maddaloni, P. De Natale, “Assessing the time constancy of the proton-to-electron mass ratio by precision ro-vibrational spectroscopy of a cold molecular beam”, *Journal of Molecular Spectroscopy* **300**, 116 (2014)
- [32] L.S. Rothman, C.P. Rinsland, A. Goldman, S.T. Massie, D.P. Edwards, J.-M. Flaud, A. Perrin, C. Camy-Peyret, V. Dana, J.-Y. Mandin, J. Schroeder, A. McCann, R.R. Gamache, R.B. Wattson, K. Yoshino, K.V. Chance, K.W. Jucks, L.R. Brown, V. Nemtchinov, P. Varanasi, “The Hitran molecular spectroscopic database and hawks (Hitran atmospheric workstation): 1996 Edition”, *J. Quant. Spectrosc. Radiat. Transfer* **60**, 665 (1998)
- [33] B. Amyay, A. Fayt, M. Herman, “Accurate partition function for acetylene, $^{12}\text{C}_2\text{H}_2$, and related thermodynamical quantities”, *J. Chem. Phys.* **135**, 234305 (2011)
- [34] Harvard-Smithsonian Center for Astrophysics (CFA), Cambridge, MA, USA; V.E. Zuev Institute of Atmospheric Optics (IAO), Tomsk, Russia: <http://hitran.iao.ru/molecule>
- [35] P. Maddaloni, M. Bellini, P. De Natale, “Laser-based Measurements for Time and Frequency Domain Applications. A Handbook.”, CRC Press, Taylor&Francis Group (2013)
- [36] G. Sanna, G. Tomassetti, “Introduction to Molecular Beam Gas Dynamics”, Imperial College Press, London (2005)
- [37] H.C. Andersen, I. Oppenheim, K.E. Shuler, G.H. Weiss, “Exact conditions for the preservation of a canonical distribution in Markovian processes”, *J. Math. Phys.* **5**, 522 (1964)
- [38] N.R. Hutzler, H.-I. Lu, J.M. Doyle, “The Buffer Gas Beam: An Intense, Cold, and Slow Source for Atoms and Molecules”, *Chem. Rev.* **112**, 4803 (2012)
- [39] M.-J. Lu, J.D. Weinstein, “Cold $\text{TiO}(X^3\Delta)$ -He collisions”, *New Journal of Physics* **11**, 055015 (2009)
- [40] S.M. Skoff, R.J. Hendricks, C.D.J. Sinclair, J.J. Hudson, D.M. Segal, B.E. Sauer, E.A. Hinds, M.R. Tarbutt, “Diffusion, thermalization, and optical pumping of YbF molecules in a cold buffer-gas cell”, *Phys. Rev. A* **83**, 023418 (2011)
- [41] B.K. Stuhl, M.T. Hummon, J. Ye, “Cold State-Selected Molecular Collisions and Reactions”, *Annu. Rev. Phys. Chem.* **65**, 501 (2014)
- [42] A. Oancea, O. Grasset, E. Le Menn, O. Bollengier, L. Bezacier, Stéphane Le Mouélic, G. Tobie, “Laboratory infrared reflection spectrum of carbon dioxide clathrate hydrates for astrophysical remote sensing applications”, *Icarus* **221**, 900 (2012)

- [43] S. Bovino, P. Zhang, V. Kharchenko, A. Dalgarno, “Relaxation of energetic S(^1D) atoms in Xe gas: Comparison of ab initio calculations with experimental data”, *J. Chem. Phys.* **135**, 024304 (2011)
- [44] G. Nan, P.L. Houston, “Velocity relaxation of S(^1D) by rare gases measured by Doppler spectroscopy”, *J. Chem. Phys.* **97**, 7865 (1992)
- [45] T.C. Onstott, D. McGown, J. Kessler, B. Sherwood Lollar, K.K. Lehmann, S.M. Clifford, “Martian CH₄: Sources, Flux, and Detection”, *Astrobiology* **6**, 377 (2006)
- [46] E. Lellouch, B. Sicardy, C. de Bergh, H.-U. Käufl, S. Kassi, A. Campargue, “Pluto’s lower atmosphere structure and methane abundance from high-resolution spectroscopy and stellar occultations”, *Astronomy&Astrophysics* **495**, L17 (2009)
- [47] L.M. Ziurys, A.J. Apponi, J.M. Hollis, L.E. Snyder, “Detection of interstellar N₂O: a new molecule containing an N-O bond”, *The Astrophysical Journal* **436**, L181 (1994)